British Journal of Anaesthesia **112** (1): 159–68 (2014)
Advance Access publication 31 July 2013 · doi:10.1093/bja/aet253

BJA

Pharmacodynamic changes with vecuronium in sepsis are associated with expression of α7- and γ-nicotinic acetylcholine receptor in an experimental rat model of neuromyopathy

L. Liu[1], S. Min[1]*, W. Li[2], K. Wei[1], J. Luo[1], G. Wu[1], L. Ao[1], J. Cao[1], B. Wang[1] and Z. Wang[1]

[1] Department of Anesthesiology, First Affiliated Hospital of Chongqing Medical University, You Yi Road 1#, Yuan Jia Gang, Chongqing 400016, China
[2] Department of Anesthesiology, Second Affiliated Hospital of Chongqing Medical University, Chongqing 400016, China
* Corresponding author. E-mail: minsu89011069@yahoo.com.cn

Editor's key points

- This study in rats demonstrates that the pharmacodynamics of non-depolarizing neuromuscular blocking agents in sepsis is associated with the expression of α7- and γ-nAChR in the skeletal muscle.
- Ulinastatin, a protease inhibitor, can improve the effects of systemic inflammation on the expression of these receptors.

Background. Resistance to non-depolarizing neuromuscular blocking agents induced by sepsis is associated with the qualitative change in the nicotinic acetylcholine receptor (nAChR). This study aims to investigate the effects of sepsis on the neuromuscular block properties of vecuronium in relation to the expression of fetal and neuronal α7 type nAChR.

Methods. Male Sprague–Dawley rats were randomly divided into sham and sepsis groups. Sepsis was induced by caecal ligation and puncture (CLP). The rats were injected i.v. with ulinastatin or normal saline on Day 10. Neuromuscular block properties of vecuronium were evaluated and neuromuscular function was assessed by electromyography on Days 1, 3, 7, and 14 after CLP. Expression of fetal and neuronal type α7-nAChR on the tibialis anterior muscle was assessed using immunohistochemistry and western blot. The mRNA encoding for γ- and α7 subunits was evaluated by real-time polymerase chain reaction.

Results. The half maximal inhibitory response of vecuronium in the sepsis group significantly increased, peaked on Day 7, and then declined on Day 14 ($P<0.05$). The neuromuscular function decreased with increasing postoperation time in the sepsis group ($P<0.05$). Sepsis significantly increased the expression of γ- and α7-nAChR along with expression of γ- and α7 subunits mRNA, peaked on Day 7, and declined on Day 14 ($P<0.05$). Ulinastatin suppressed the expression of receptor protein and mRNA encoding for γ- and α7 subunits ($P<0.05$).

Conclusions. Pharmacodynamic changes with vecuronium seem to be associated with the expression of γ- and α7-nAChR in the skeletal muscle. Ulinastatin can improve this effect by inhibiting the expression of these receptors.

Keywords: neuromuscular blocking agents; pharmacology; receptors, nicotinic; sepsis

Accepted for publication: 28 May 2013

Non-depolarizing neuromuscular blocking agents (NMBAs) are frequently used for the management of septic patients who require mechanical ventilation during anaesthesia and intensive care.[1] Sepsis attenuates the intensity of the neuromuscular blocking effect of NMBAs.[2 3] Thus, elucidating the pathogenic mechanism by which sepsis alters the pharmacodynamics of NMBAs is useful to determine appropriate doses for the safe use of NMBAs.

The altered responses to NMBAs are associated with quantitative or qualitative changes on nicotinic acetylcholine receptors (nAChRs).[4–6] Martyn and colleagues first reported on the resistance to the neuromuscular effects of NMBAs after burns, immobilization, and denervation.[7–9] Some possible mechanisms have been revealed, including plasma protein binding, muscle atrophy, and up-regulation of nAChRs. Interestingly, similar pharmacodynamic changes in NMBAs also occurred in septic patients. However, quantitative increases of nAChR have not been observed in septic muscles.[10–12] Whether qualitative changes occur in nAChRs is still unknown. Three variants of post-junctional nAChRs have been identified: adult- (ε-nAChR), fetal- (γ-nAchR), and neuronal α7 type (α7-nAchR). Normally, only ε-nAChR is synthesized in muscle cells and is anchored to the end-plate membrane, which maintains the neuromuscular transmission function. In the early fetal stage, two other isoforms, the γ- and α7-nAChR, are scattered throughout the muscle membrane before innervation.[5 13–15] Denervation and some other pathological states (e.g. burn and immobilization) lead to the re-expression of γ- and α7-nAChR.[15 16] These receptors alter drug sensitivity.[17 18] Ulinastatin, a protease inhibitor purified from human urine, has anti-inflammatory effects[19 20] and increases the release of acetylcholine at the neuromuscular

junction.[21] Acetylcholine-induced electrical activity suppresses the expression of α7- and γ-nAChR. Thus, we hypothesized that the expression of α7- and γ-nAChR can be improved by ulinastatin treatment.

This study in rats tested the hypothesis that the expression of α7- and γ-nAchR on the septic muscle attenuates the muscle-relaxing effect of NMBAs. We used surgical peritonitis to induce a sepsis model avoiding steroid use or surgical denervation to investigate the alteration of neuromuscular block properties of vecuronium, a non-depolarizing NMBA. We also assessed neuromuscular function in relation to mRNA encoding for the γ- and α7 subunits of acetylcholine receptor and for the expression of protein receptors.

Methods

Animals

Male Sprague–Dawley rats (age: 2–3 months, weight range: 200–220 g) were obtained from the Experimental Animal Centre of Chongqing Medical University (Chongqing, China). All rats received humane care according to the Care and Use Committee of Chongqing Medical University. One week before the experiments, the rats were housed in a specific pathogen-free laboratory in an acclimatized room at standard room conditions [25 (2)°C, 55% humidity] with a 12 h light/dark cycle. The rats were given free access to water and standard chow. All experimental procedures involving animals were approved by the Animal Ethics and Use Committee of Chongqing Medical University.

Anaesthesia and vital parameters

For neuromuscular functional and pharmacological studies, the animals were anaesthetized with 10% chloral hydrate [350 mg kg^{-1} intraperitoneal (i.p.)] on the day of the experiment. The animals were tracheotomized, and their lungs were mechanically ventilated. The mean arterial pressure, heart rate and body temperature (°C) were continuously monitored. Pa_{O_2}, Pa_{CO_2}, and acid–base status were intermittently measured and corrected to ensure stable haemodynamic conditions. The rats were excluded from the experiment if haemodynamically unstable (mean arterial pressure <10.7 kPa) or if the blood gas level was not within the range [Pa_{O_2} >13.3 kPa; pH 7.36–7.44; Pa_{CO_2} 4.8–5.8 kPa; base excess of −2 (2) mEq].

Animal models and group assignments

For surgical intervention, the rats were anaesthetized with i.p. administration of 10% chloral hydrate (350 mg kg^{-1}). All the rats were weighed daily and randomly divided into two groups: (i) the sepsis group in which caecal ligation and puncture (CLP) was performed; and (ii) the sham group in which a sham operation was performed (n=6). Given the time frame of the sepsis model, the rats in the sepsis group were assigned to four subgroups: Day 1 (n=6), Day 3 (n=6), Day 7 (n=12), and Day 14 (n=24). After 10 days of CLP, the rats in the sepsis group were i.v. injected with ulinastatin (5000 U kg^{-1}) (n=12) or 0.9% normal saline (NS) (n=12). The group assignments are shown in Figure 1.

In the sepsis group, sepsis was induced by CLP, which was performed as described previously.[22] In this sepsis model, the rats were considered septic at 6 h after CLP.[23] Midline laparotomy was performed to expose the caecum. The caecum was ligated tightly with a 3-0 silk suture at its base below the ileocaecal valve and punctured with a 24-gauge needle avoiding bowel obstruction. A small amount of faeces was exteriorized by gentle pressure applied on the ligated caecum. Then, the caecum was returned to the peritoneal cavity. The abdomen was closed with 3-0 silk. The rats in the sham group received

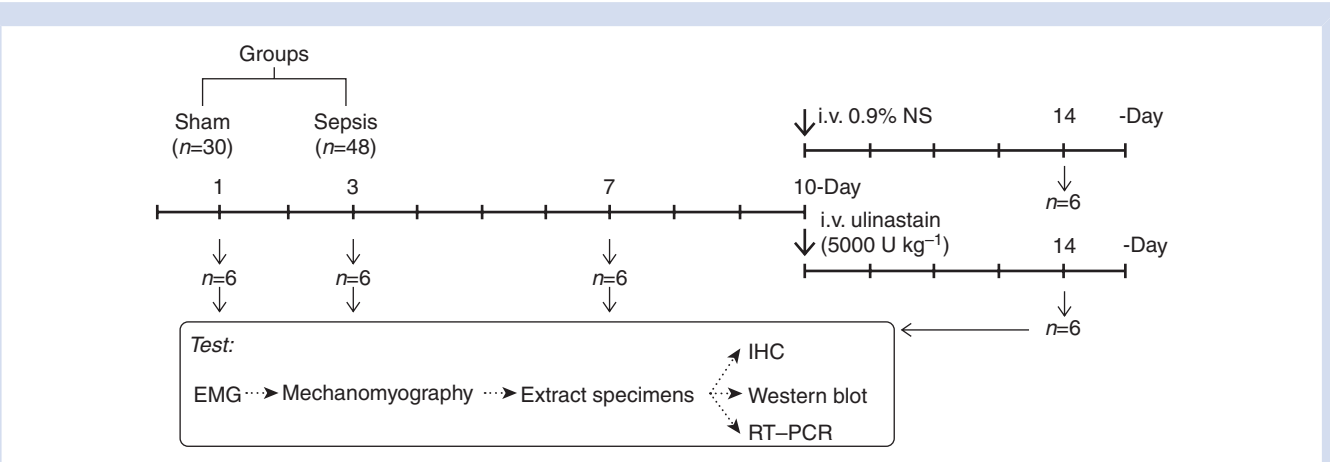

Fig 1 A flow diagram of the experiments. A total of 48 rats were assigned to the sepsis groups (Day 1, n=6; Day 3, n=6; Day 7, n=12; Day 14, n=24) and 30 rats were assigned to the sham groups (Day 1, n=6; Day 3, n=6; Day 7, n=6; Day 14, n=6). The rats in the Day 14 group were divided into two subgroups: 0.9% NS (n=12) and ulinastatin (n=12). Given the exclusion of 19 rats because of death or haemodynamic and metabolic instability, the final statistical analysis included 29 animals in the sepsis groups.

the same anaesthesia and surgical manipulation without CLP. Immediately after surgery, each rat received once paracetamol (100 mg kg^{-1} i.p.), antibiotic primaxin (25 mg kg^{-1} i.p., Merck), and 0.9% NS (10 ml kg^{-1} i.p.), and was rewarmed for ~3 h. Primaxin is a mixed formulation composed of imipenem (*N*-formimidoylthienamycin monohydrate) and cilastatin sodium. It is a commonly used antibiotic that could elevate the survival of septic animal models constructed by CLP.

Evaluation of neuromuscular function

Electromyographic (EMG) recordings were measured at pre- and post-modelling. The data were obtained from the right sciatic nerve that was stimulated supramaximally (intensity, 3 V; duration, 0.2 ms; and frequency, 1 Hz) by a direct stimulation electrode (RM6240 Systems, Inc., Cheng Du, China) from the sciatic nerve. Compound muscle action potential (CMAP) was recorded using a superficial disc electrode located on the tibialis anterior muscle before and at different times after surgery, as described previously.[24] Electromyographical analysis used the RM6240USB2.0S (I) version 1.0.2 software (RM6240 Systems, Chengdu Instrument Company, Chengdu, China), with amplitude, and duration of CMAP as the parameters. The motor conduction velocity (MCV) was calculated as the distance of conduction/latency time. The temperature of each rat was kept at ~36–37°C using a heating light. Neuromuscular dysfunction was defined as a decrease of ≥20% of the lower limit of the normal CMAP amplitude.[25 26]

Pharmacodynamics of vecuronium

Neuromuscular block was monitored by evoked mechanomyography using a nerve stimulator (RM6240 Systems) and a RM6240-JZJ100 force transducer (RM6240 Systems). The rats were placed in the dorsal recumbent position. The tendon of the tibialis anterior muscle on each side (left or right side by random selection) was surgically exposed, severed, and then individually attached to separate transducers. Both sciatic nerves were exposed at the thigh. Stimulation electrodes were attached to measure nerve-mediated contraction of the tibialis anterior muscle. To ensure a force vector control, we stabilized each knee rigidly with a clamp. A preload of 30 g was applied to yield maximal isometric contractions. The nerve-evoked tensions of the respective tibialis anterior muscles were recorded by an amplifier and displayed using the RM6240USB2.0S (I) version 1.0.2 software.

The isometric twitch tension of the tibialis anterior muscle was estimated by researchers who were blinded from the experimental group of each specimen. Twitch tension was elicited by indirect supramaximal constant current stimulation at 0.1 Hz using a stimulator and a constant-current unit to deliver twitch tension. All forces were measured in grams. After the elicited twitch tension was stabilized, single-twitch tension (averaged in groups of five) was determined. The potency of vecuronium was tested using the cumulative dose–response method. Bolus doses of vecuronium were administered i.v. in increments of 0.05–1 mg kg^{-1} until the twitch height achieved maximal depression. Each incremental dose was given only after the twitches were allowed to recover to baseline values. The twitch tension inhibitory effect was normalized by the following equation: % inhibition$=100\times(1-A/B)$, where A represents the minimal twitch height in the presence of vecuronium and B is baseline values of twitch height. Dose–response analysis: inhibitory effect *vs* dose data was fitted using a four-variable logistic sigmoidal dose–response model. The expression relating the dose to the inhibitory effect is as follows:

$$Y=\left[\mathrm{START}+(\mathrm{END}-\mathrm{START})\frac{x^n}{(IC_{50})^n+x^n}\right]\times 100\%$$

where Y represents the fraction of inhibition, START refers to Y for the minimal response, END is Y for the maximum response, n is the Hill coefficient (considered as a slope parameter), x is the administered dose, and 50% inhibitory concentration (IC_{50}) is the effective dose eliciting 50% of the maximal effect.

Tissue preparation

The animals were humanely killed by deep anaesthesia with sodium pentobarbital (65 mg kg^{-1} i.p.), the tibialis anterior muscle specimens of rats were collected in 4% paraformaldehyde or liquid nitrogen.

Immunohistochemistry

Immunostaining was performed using the streptavidin–peroxidase method. For detection of α7-nAchR, the muscle specimens were immediately fixed with 4% paraformaldehyde in phosphate buffer saline (PBS) and embedded in paraffin. Another muscle specimens were collected in liquid nitrogen and were fixed in cold acetone for 1~2 min. The endogenous peroxidase was inactivated by incubating the tissue sections in 3% hydrogen peroxide for 30 min at 25°C. The sodium citrate buffer (0.01 mol $litre^{-1}$, pH 6.0) was used to retrieve antigen at 96–98°C for 10 min. Then, the rabbit anti-nAChR α7 pAb (ab10096, Abcam Ltd, dilution 1:800) was added into a humidity chamber and was incubated with samples at 4°C overnight. For detection of γ-nAchR, the muscle specimens were collected in liquid nitrogen. Tissue sections were fixed in cold acetone for 1~2 min and rehydrated in PBS. The anti-nAChR γ pAb (LS-C73537, LSBio, Inc., dilution 1:1000) was applied to the tissue sections. Then following anti-rabbit (for α7-nAchR) or -mouse (for γ-nAchR) IgG secondary antibodies were used to detect each primary antibody. The sections were routinely counterstained with haematoxylin. Controls consisted of unstained and secondary antibody alone sections where all, or just the primary, antibodies were replaced with dilution buffer. The average optical density was analysed in 10 randomly selected microscopic fields in five sections of each group at a 400-fold magnification.

Western blot analysis

Tissues were homogenized using lysis buffer (Beyotime, China), and supernatants were collected after centrifugation at 12 000×*g* for 15 min at 4°C. After quantitative analysis of protein concentration, total proteins were separated by

sodium dodecyl sulphate–polyacrylamide gel electrophoresis, transferred to polyvinylidene fluoride membranes (Millipore, Billerica, MA, USA), blocked with 5% non-fat milk in Tris-buffered saline for 1 h at 37°C, and then incubated overnight at 4°C with sc-13998 (Santa Cruz, Inc., dilution: 1:500) and ab10096 (1:1000) as primary antibodies. After incubation for 1 h at 37°C with secondary antibody (1:2000; Beyotime), bands were seen using the enhanced chemilumine-scence kit (Beyotime) according to the manufacturer's protocol. All results were normalized to glyceraldehyde-3-phosphate dehydrogenase (GAPDH) levels.

Real-time polymerase chain reaction analysis

The mRNA encoding for γ- and α7 subunits are CHRNG and CHRNA7, respectively. Total cellular RNA was isolated from the tibialis anterior muscle with TRIzol (Invitrogen, Carlsbad, CA, USA) according to the manufacturer's instructions. Real-time quantitative polymerase chain reaction (PCR) was performed using iQ SYBR Green Supermix on the iCycler iQ detection system (Bio-Rad, Hercules, CA, USA). The standard reaction volume was 20 μl and contained 1 μl QuantiTect SYBR Green PCR Master Mix (Qia-gen, Valencia, CA, USA), 0.1 U AmpErase uracil N-glycosylase (UNG) enzyme (PE Biosystems, Foster City, CA, USA), 0.7 μl cDNA template, and 0.25 μM forward and reverse primers. The initial step of PCR was 2 min at 50°C for AmpErase UNG activation, followed by a 15 min hold at 95°C. The reverse transcriptase (RT)–PCR programme on iCycler was 95°C for 15 s, 60°C for 30 s, and 72°C for 30 s. All experiments were confirmed with three animals. The expression levels for each gene of interest were calculated by normalizing the quantified mRNA amount to the quantified mRNA amount of GAPDH. Primers for γ and α7 genes were designed using the Primer Express software (Perkin-Elmer, Foster City, CA, USA). Primer sequences are given in Table 1.

Statistical analysis

Competition analysis data [IC_{50} and slope at IC_{50}] were determined from a four-variable logistic sigmoidal dose–response model fitted to the dose–response curves with Prism 4 (GraphPad Software, Inc., San Diego, CA, USA). Data on twitch tension inhibition rate were expressed as mean (SEM). IC_{50} values were expressed as means with 95% confidence intervals, whereas the IC_{50} ratio and slope at log IC_{50} were expressed as mean (SD). The IC_{50} ratio was defined as the IC_{50} of the dose–response curve in the sepsis group divided by that in the sham group. The remaining data were expressed as mean (SD). Real-time PCR data analysis was performed using the Q-Gene software, which expresses data as mean normalized expression (MNE). MNE is directly proportional to the RNA amount of the target gene relative to the RNA amount of the reference gene. Statistical significance was assessed using one-way repeated-measures analysis of variance (ANOVA) followed by ANOVA with the Scheffé *F*-test. A *P*-value of <0.05 was considered to indicate statistical significance.

Results

Mortality, behaviour, and weight gain

No deaths occurred in the sham-operated rats ($n=30$). All deaths associated with CLP occurred after 5 days after laparotomy. The mortality rates were 25% (3 in 12 rats) on Day 7, 41% (5 in 12 rats) on Day 14 for 0.9% NS, and 33% (4 in 12 rats) on Day 14 for ulinastatin after CLP. Almost all of the CLP animals demonstrated crouching, piloerection, decreased spontaneous locomotor activity, and exudation around the eyes from Day 1 to Day 3 after laparotomy. From Day 6 to Day 7, 14 rats progressed to septic shock and 12 rats to death. The rats with septic shock were immobilization and showed motor restlessness, hair erection, and subconjunctival haemorrhage. At necropsy of the dead animals, the peritoneal cavity contained a large amount of bloody and malodorous fluid, and the caecum was distended and gangrenous. Only three rats did not exhibit the symptoms described above. Surviving CLP rats developed diarrhoea and failed to gain weight. From Day 9, the animals gained weight in parallel to that of the sham rats. However, decreased spontaneous locomotor activity and ruffled fur visually distinguished the CLP rats from the sham rats throughout the observation period.

Electrophysiological recordings

The CMAP recorded for each group is shown in Figure 2A. In the sham group, the amplitude of CMAP was 16.51 (2.53) mV. However, in the sepsis group, the amplitudes of CMAP decreased significantly, and the peak appeared on Day 7 post-operation ($P<0.01$; Fig. 2B). The duration of CMAP in the sepsis group was prolonged significantly, and the peak appeared on Day 7 post-operation ($P<0.01$). No significant difference was found between the duration of CMAP in the Day 14 group and that in the ulinastatin group ($P>0.05$; Fig. 2C). The nerve conduction velocity significantly decreased in the sepsis group compared with that in the sham group ($P<0.05$). The peak appeared on Day 7. The nerve conduction velocity recovered slightly after ulinastatin administration ($P<0.01$; Fig. 2D). In the sepsis group, the twitch tension magnitudes elicited by continuous stimulations were the largest in the Day 1 group, second largest in the Day 3 group, and smallest in the Day 14 group ($P<0.05$). No significant difference was found between

Table 1 Primer sequences for γ- and α7 subunits of nAChR

	Forward	Reverse
γ subunit	5′-GGGCCGAGTGCTGGACCG-3′	5′-GGCGGGGGTCTCCAGGGA-3′
α7 subunit	5′-GGCCCGGAGAGGACAAGG-3′	5′-CGGCCACATACGACCCCA GAGT-3′

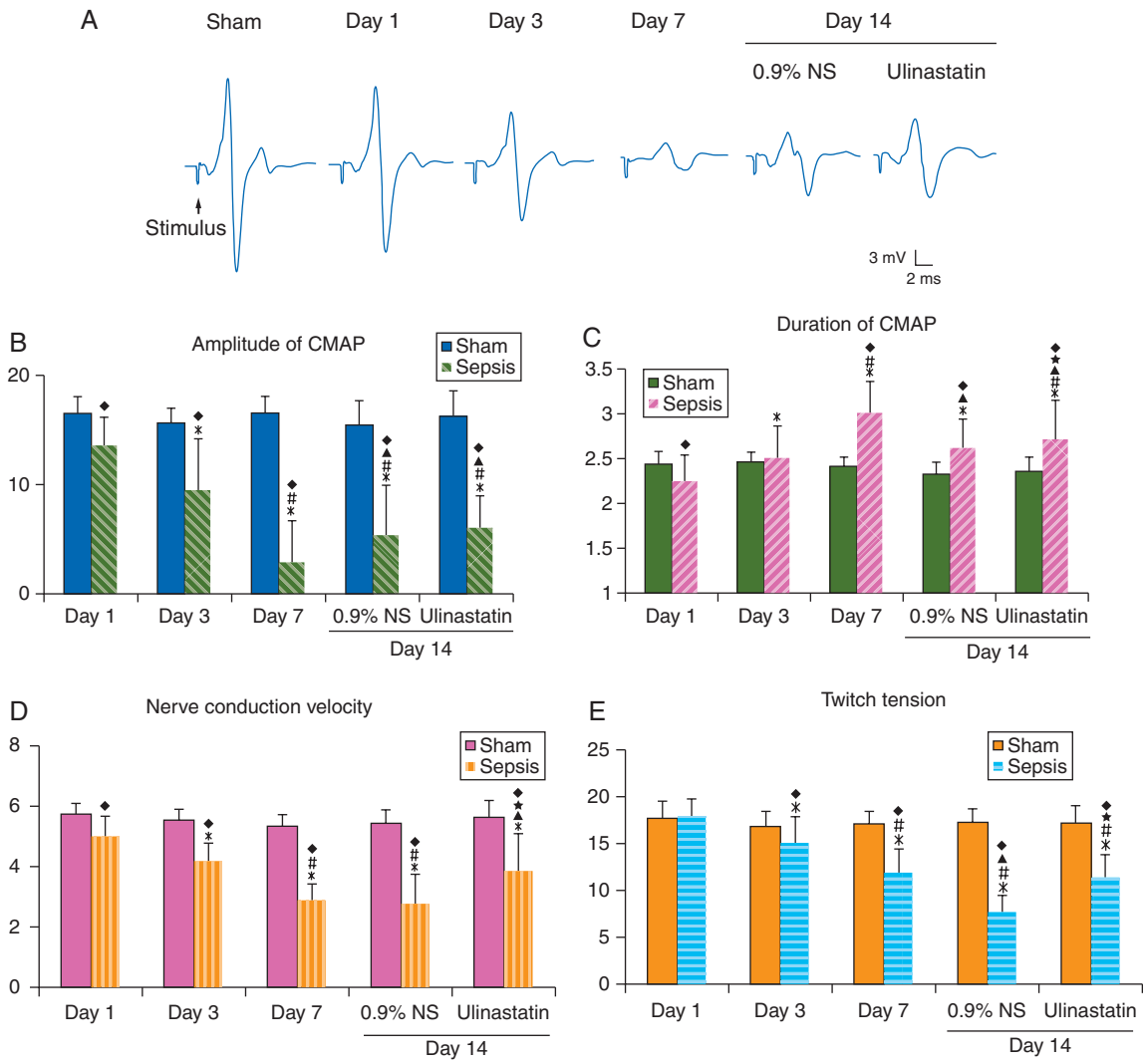

Fig 2 EMG recording results. (A) Samples of the CMAPs recorded after CLP in each group, (B) amplitudes, (C) durations, (D) MCV of the sham and sepsis groups regarding time, and (E) single-twitch tension elicited by indirect stimulation. *$P<0.05$ *vs* Day 1; $^{\#}P<0.05$ *vs* Day 3; $^{\blacktriangle}P<0.05$ *vs* Day 7; $^{\bigstar}P<0.05$ *vs* 0.9% NS in the Day 14 group; and $^{\blacklozenge}P<0.05$ *vs* the sham group.

the twitch tension elicited by stimulation in the Day 7 group and that in the ulinastatin group ($P>0.05$; Fig. 2E).

Vecuronium dose–response curves

Vecuronium reduced the magnitudes of indirectly elicited twitch tensions in a dose-dependent manner ($P<0.01$; Fig. 3). Fitting the vecuronium dose–response data to the four-variable logistic equation yielded IC_{50} values, which quantitatively indicate the position of the curve. The IC_{50} of vecuronium gradually increased from Day 1 to Day 14 in the sepsis group ($P<0.01$; Table 2). However, the IC_{50} of vecuronium in the rats with ulinastatin was significantly lower than that in the rats with 0.9% NS in the Day 14 group ($P<0.01$). It was close to the IC_{50} of the Day 7 group ($P>0.01$). The IC_{50} ratio, which standardizes the magnitudes of the rightward shifts of the dose–responses curves, was significantly the largest for the rats with 0.9% NS, second largest for the rats in the ulinastatin and Day 7 groups, and smallest on Days 1 and 3 in the sepsis group ($P<0.01$). The slope at IC_{50}, which characterizes the slope of the curves, was not significantly different between the sham and Day 1 in the sepsis group ($P>0.05$). In the sepsis group, the slope at IC_{50} gradually increased from Day 1 to Day 3 in the sepsis group ($P<0.01$). The slope at IC_{50} for the rats with 0.9% NS was significantly less than that of the rats with ulinastatin in the Day 14 group ($P<0.01$; Table 2).

Immunohistochemical staining

In the sham muscle specimens, γ- and α7-nAChR stains were not observed in the skeletal muscle membrane. In the septic

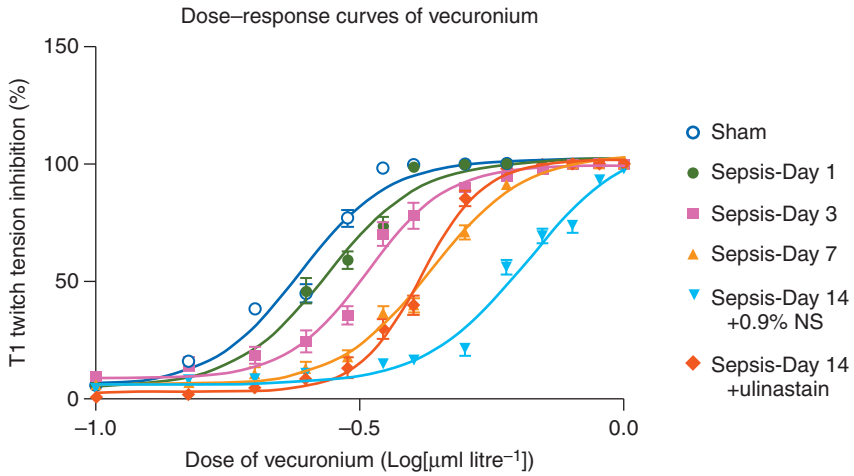

Fig 3 Dose–response curves of vecuronium in the sham, Day 1, Day 3, Day 7, Day 14+0.9% NS, and Day 14+ulinastatin groups. Twitch tension was elicited by indirect stimulation at 0.1 Hz. The *x*-axis represents the logarithm of the vecuronium concentration. Each point represents the mean (SEM) of the percentage of twitch tension inhibition. The dose–response curves of these experimental groups were significantly different for vecuronium ($P<0.05$, each by Scheffé *F*-test). The dose–response curves of the sepsis groups were significantly different from those of the sham group ($P<0.01$, each by Scheffé *F*-test). No significant difference was found between the curves of the Day 14+ulinastatin group and those of the Day 7 group ($P>0.05$, Scheffé *F*-test).

Table 2 IC_{50} values, IC_{50} ratio, and slopes of the vecuronium dose–response curves. IC_{50}=50% inhibitory dosage. IC_{50} ratio=(IC_{50} of the sepsis group dose–response curves/IC_{50} of the sham group dose–response curve). IC_{50} values and slopes at IC_{50} are expressed as means with 95% confidence intervals (μmol litre^{-1}) and mean (SE). *$P<0.05$ *vs* the sham group; $^{\#}P<0.01$ *vs* Day 1 in the sepsis group; $^{\star}P<0.05$ *vs* Day 3 in the sepsis group; $^{\blacktriangle}P<0.05$ *vs* Day 7 in the sepsis group; $^{\blacklozenge}P<0.05$ *vs* Day 14 of 0.9% NS in the sepsis group

	Sham	Sepsis				
		Day 1	Day 3	Day 7	Day 14	
					0.9% NS	Ulinastatin
IC_{50}	0.24 (0.23–0.25)	0.27 (0.26–0.28)	0.32* (0.31–0.34)	$0.43^{\#\star}$ (0.42–0.44)	$0.65^{\#\star\blacktriangle}$ (0.61–0.71)	$0.41^{\#\star\blacklozenge}$ (0.40–0.42)
Hillslope	5.17 (0.42)	5.68 (0.53)	5.77 (0.62)*	$4.97\ (0.34)^{\#\star}$	$4.49\ (0.51)^{\#\star\blacktriangle}$	$7.30\ (0.57)^{\#\star\blacktriangle\blacklozenge}$
IC_{50} ratio	–	1.04 (0.95–1.16)	1.33* (1.05–1.88)	$1.79^{\#\star}$ (1.24–2.32)	$2.71^{\#\star\blacktriangle}$ (2.34–3.07)	$1.71^{\#\star\blacklozenge}$ (1.41–1.98)

muscle specimens, the skeletal muscle membrane showed γ- and α7-nAChR immunoreactivity from Day 1 to Day 14 (Fig. 4A). On Day 14, the number of γ- and α7-nAChR on the skeletal muscle membrane peaked by positive immunostaining with anti-nAChR γ antibody and anti-nAChR α7 antibody (Fig. 4B). After ulinastatin administration, the expression levels of γ- and α7-nAChR decreased in the skeletal muscle membrane on Day 14, compared with those on Day 7 ($P<0.05$).

Western blotting and RT–PCR

The relative protein levels to GAPDH of γ- and α7-nAChR significantly increased on Days 1, 3, 7, and 14 in the sepsis group compared with those in the sham group. The peak value appeared on Day 7 and 14 post-procedure for γ- and α7-nAChR, respectively, by semi-quantitative analysis ($P<0.05$; Fig. 5).

The γ- and α7 subunits of mRNA were detected in all muscle samples by RT–PCR. Similar to the results of western blot, the ratio of γ- and α7-mRNA to GAPDH mRNA significantly increased on Days 1, 3, 7, and 14 in the sepsis group compared with that in the sham group. The peak value appeared on Day 7 and 14 post-procedure for γ- and α7-nAChR, respectively ($P<0.05$; Fig. 6).

Correlation between IC_{50} of vecuronium and γ-nAchR, or α7-nAchR protein

Statistically significant positive correlations were found between the IC_{50} of vecuronium and γ-nAchR protein level in the sepsis group ($r=0.864$, $P=0.026$). The level of α7-nAchR protein was correlated positively with the IC_{50} of vecuronium in the sepsis group ($r=0.765$, $P=0.002$).

Discussion

The results of this study demonstrated that sepsis results in resistance to the neuromuscular effect of vecuronium. This

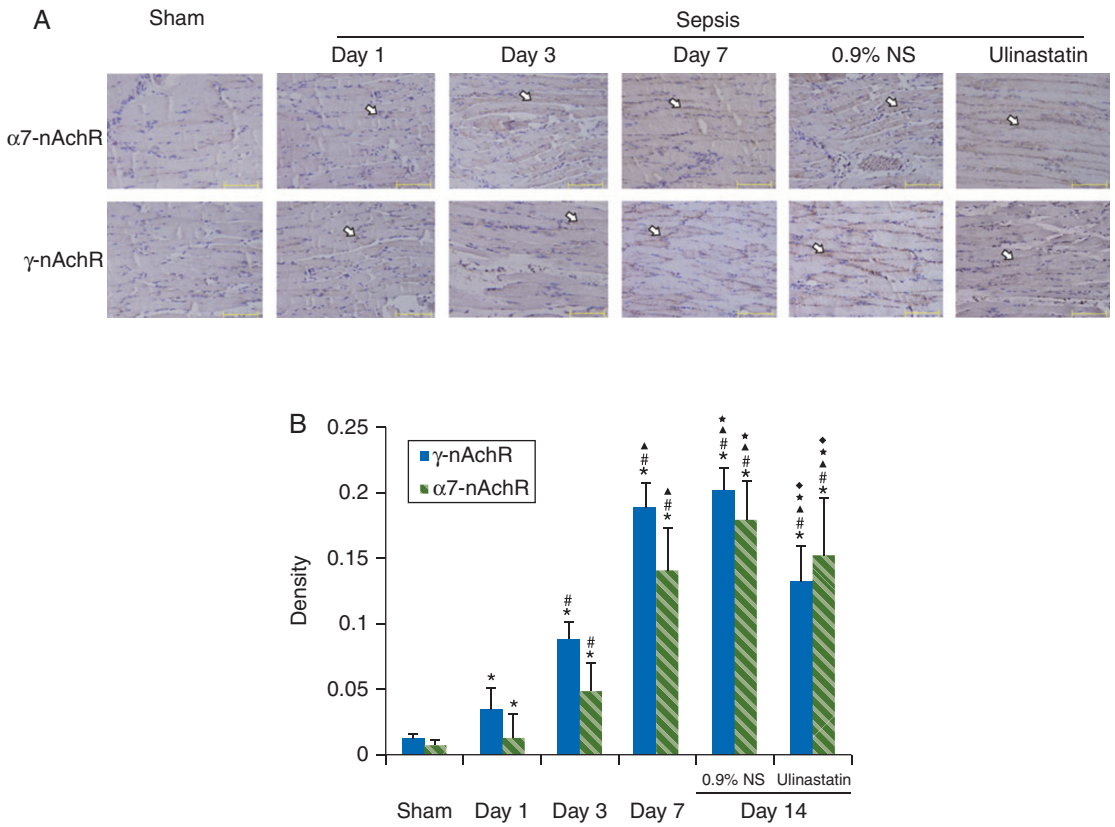

Fig 4 Immunohistochemical staining of γ- and α7-nAChR in the tibialis anterior muscle samples (A, scale bar=20 μm). The expression of γ- and α7-nAChR were detected on the skeletal muscle membrane, which appeared on Day 1, peaked on Day 7, and declined on Day 14 after ulinastatin administration. An average optical density of γ- and α7-nAChR is shown in graph (B). All values are expressed as mean (SD) (n=6). *P<0.05 *vs* Day 1; #P<0.05 *vs* Day 3; ▲P<0.05 *vs* Day 7; ★P<0.05 *vs* 0.9% NS in the Day 14 group; and ◆P<0.05 *vs* the sham group.

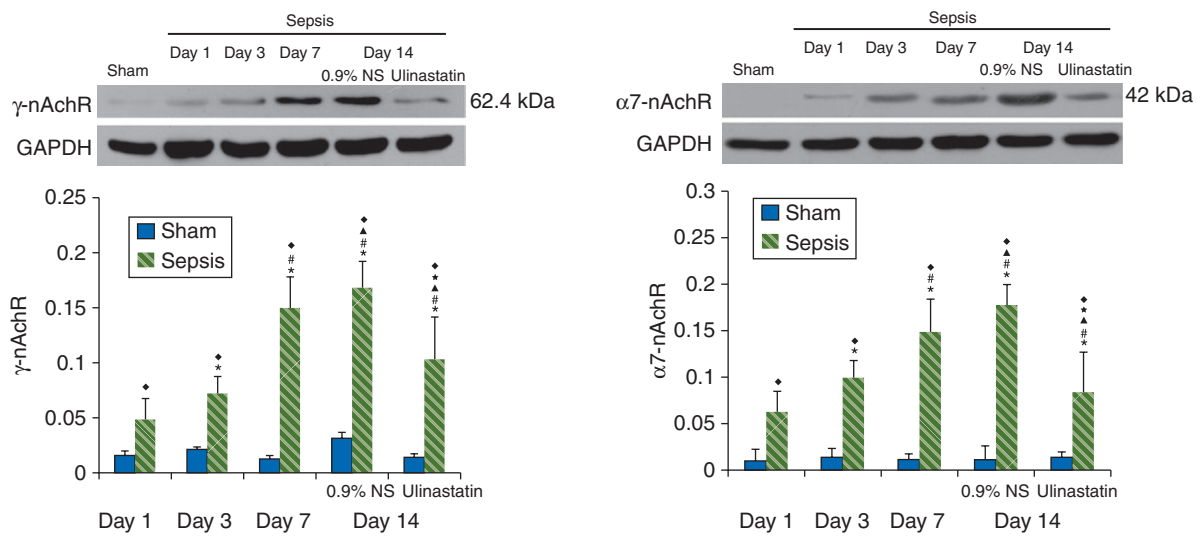

Fig 5 Western-blot analysis of γ-nAChR (A) and α7-nAChR (B) protein from the tibialis anterior muscle specimens. Representative results from three individual animals are shown. Relative intensity of γ- or α7-nAChR to GAPDH is shown in the graphs. All values are expressed as mean (SD) (n=6). *P<0.05 *vs* Day 1; #P<0.05 *vs* Day 3; ▲P<0.05 *vs* Day 7; ★P<0.05 *vs* 0.9% NS in the Day 14 group; and ◆P<0.05 *vs* the sham group.

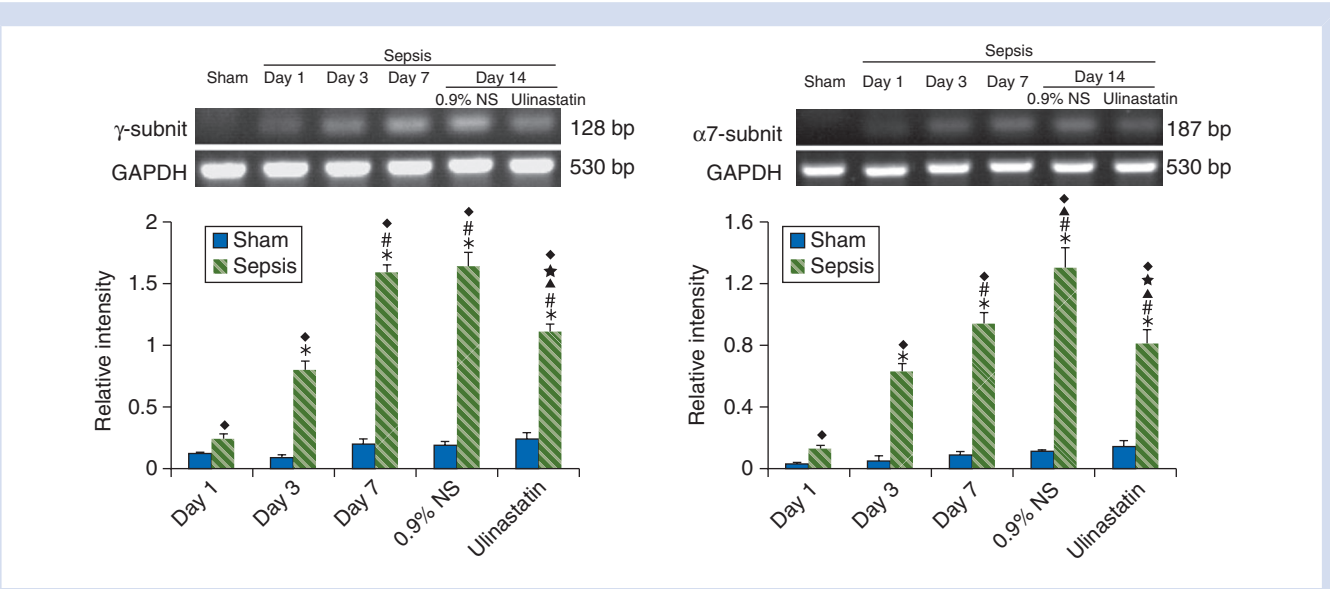

Fig 6 Analysis of γ-nAChR (A) and α7-nAChR (B) mRNA expression from the tibialis anterior muscle specimens by RT–PCR. Representative results from three individual animals are shown. Relative intensity of γ- or α7-nAChR to GAPDH is shown in the graphs. All values are represented as mean (SD) ($n=6$). *$P<0.05$ *vs* Day 1; #$P<0.05$ *vs* Day 3; ▲$P<0.05$ *vs* Day 7; ★$P<0.05$ *vs* 0.9% NS in the Day 14 group; and ◆$P<0.05$ *vs* the sham group.

resistance manifested itself as early as Day 3 after CLP operation, persisted until Day 7, and recovered to some extent after ulinastatin administration. This resistance is related to qualitative (isoform) changes in the receptor. These receptors have different electrophysiological properties and ligand-specific sensitivity or affinity. This study has documented a relation between expression of α7- and γ-nAchR and resistance to NMBAs.

We used a septic neuromyopathy model that is considered to be more appropriate to study the physiopathology of neuromuscular disorders.[27 28] CLP-induced sepsis is characterized by a hyperdynamic state in the early phase (the first 5 days after CLP) followed by a hypodynamic state in the chronic phase (6–28 days after CLP) in the laboratory. It is considered more relevant to clinical sepsis.[29–31]

It has been reported that acute sepsis stage-dependently attenuated the effect of NMBAs.[32] However, the effect of chronic sepsis on NMBAs is still unclear. In the endotoxin model of repeated i.p. injections of lipopolysaccharide into mice, Tomera and Martyn[33] reported a three-fold shift to the right of the dose–response curve of d-tubocurarine after 2 weeks. In this study, the rightward-shift magnitudes of the dose–response curves of vecuronium increased about three-fold at 14 days after CLP. Nevertheless, the rightward shift can be reversed partially by ulinastatin administration. The results suggest that systemic inflammation is an important factor, resulting in resistance to NMBAs in sepsis.

The mechanisms of sepsis-induced resistance to NMBAs include increased binding of NMBAs to α1-acid glycoprotein (AAG)[11] and facilitated endplate potentials.[34] AAG is a second-phase acute phase protein, which was primary protein binding to NMBAs. Its serum concentration increases ~48 h after tissue injury. And this change reaches a maximum after 3–4 days and slowly declines during the next 10–14 days. Fink and colleagues reported that resistance to atracurium during systemic inflammation is attributable to increased drug binding to AAG. They used an a-bungarotoxin to quantitate the nAChRs. Nevertheless, this ligand does not differentiate nAChRs in muscles.[4 35] Kim and colleagues[36] demonstrated the capacity of AAG binding to NMBAs, which was significant but limited. Martyn's group reported resistance to neuromuscular blockade induced by NMBAs in burned and trauma was related to up-regulation of nAChRs. Elevated plasma binding did not explain the potentiating effect of resistance to NMBAs.[7 16 37] In our study, γ- and α7-nAChR were found on the skeletal muscle membrane by molecular biological and immunological techniques. The levels of these receptors were highly correlated with the IC_{50} of the dose–response curves of vecuronium. These results suggested that sepsis-induced hyposensitivity to NMDAs was associated with changes in the quality of post-junctional nAChR. The reduced slope of dose–response curves in septic rats also indicated that sepsis altered the affinities of nAChR to NMDAs, which also originated from quality alteration of nAChR. Thus, different pharmacokinetic and pharmacodynamic factors can potentially contribute to this resistance.

Compared with ε-nAChR, 1/10th – 1/100th doses of agonists affect depolarization in the γ-nAChR.[18 38 39] Low antagonist concentration effectively antagonizes the actions of iontophoretically applied Ach in nAChR.[17] α7-AChR has a lower affinity for antagonists. Chiodini and colleagues[40] investigated the effects of atracurium on α7-nAChR by biochemical and electrophysiological methods. A comparable inhibition of acetylcholine-evoked current for α7-nAChR was rapid and readily reversible. Higher concentrations of these drugs were required to block α7-AChR than ε-nAChR.[41] Thus, γ- and

α7-nAChR expressed on the muscle membrane can lead to lower affinity for NMBAs, thus requiring higher concentration of these drugs for inhibition.

The preliminary indirect evidence indicated that inflammatory cytokines and magnesium can produce a 'denervation-like state'.[42] The denervation-like state of the skeletal muscle induces an expression of heterogeneous nAChR.[16 43] Compared with denervation, the denervation-like state can be considered a state of dysfunction. In our study, we found that sepsis damaged function of motor nerve, including CMAP amplitude of and decreased MCV.

Ulinastatin, a protease inhibitor, was administered to septic rats. Ulinastatin can improve resistance to vecuronium induced by sepsis and inhibit the expression of heterogeneous nAChRs. The effects of ulinastatin included two aspects: (i) ulinastatin inhibit proinflammatory cytokine release, especially TNF-α and IL-6, which serve as moderators of muscle dysfunction and cytokine-mediated muscle damage;[44 45] and (ii) the nerve-induced electrical activity suppresses the expression of α7- and γ-nAChR.[46] Ulinastatin increases acetylcholine release at the neuromuscular junction and enhances neuromuscular electrical activity.[21]

In summary, this study demonstrates that the pharmacodynamics of NMBA changes in sepsis is associated with the expression of α7- and γ-nAChR in the skeletal muscle. Ulinastatin can improve the effects of systemic inflammation on the expression of these receptors.

Authors' contributions

L.L. contributed to the design of the experimental protocol and participated in the establishment of the animal model, pharmacodynamic testing, and data analysis. L.L. and Z.W. prepared the manuscript. W.L. contributed to the design of the experimental protocol and participated in the data collection. K.W. and J.C. contributed to the electrophysiological testing and data interpretation. J.L. and L.A. performed immunohistochemical staining and molecular biological detection. B.W. and G.W. contributed to the data analysis. S.M. approved the final manuscript. K.W., J.C., and L.L. attest to the integrity of the original data and the analysis reported in this manuscript. L.L. is the archival author.

Declaration of interest

None declared.

Funding

This study was supported by funds from the National Key Clinical Specialist of Ministry of Public Health, the Medical Key Subjects in Chongqing province, and Wu Jie Ping Medical Science Foundation of China.

References

1 Gehr LC, Sessler CN. Neuromuscular blockade in the intensive care unit. *Semin Respir Crit Care Med* 2001; **22**: 175–88

2 Liu X, Kruger PS, Weiss M, Roberts MS. The pharmacokinetics and pharmacodynamics of cisatracurium in critically ill patients with severe sepsis. *Br J Clin Pharmacol* 2012; **73**: 741–9

3 Narimatsu E, Niiya T, Kawamata M, Namiki A. Sepsis stage dependently and differentially attenuates the effects of nondepolarizing neuromuscular blockers on the rat diaphragm in vitro. *Anesth Analg* 2005; **100**: 823–9

4 Martyn JA, White DA, Gronert GA, Jaffe RS, Ward JM. Up-and-down regulation of skeletal muscle acetylcholine receptors. Effects on neuromuscular blockers. *Anesthesiology* 1992; **76**: 822–43

5 Martyn JA, Richtsfeld M. Succinylcholine-induced hyperkalemia in acquired pathologic states: etiologic factors and molecular mechanisms. *Anesthesiology* 2006; **104**: 158–69

6 Dodson BA, Kelly BJ, Braswell LM, Cohen NH. Changes in acetylcholine receptor number in muscle from critically ill patients receiving muscle relaxants: an investigation of the molecular mechanism of prolonged paralysis. *Crit Care Med* 1995; **23**: 815–21

7 Hogue CW Jr, Itani MS, Martyn J. Resistance to d-tubocurarine in lower motor neuron injury is related to increased acetylcholine receptors at the neuromuscular junction. *Anesthesiology* 1990; **73**: 703–9

8 Ibebunjo C, Nosek MT, Itani MS, Martyn JA. Mechanisms for the paradoxical resistance to d-tubocurarine during immobilization-induced muscle atrophy. *J Pharmacol Exp Ther* 1997; **283**: 443–51

9 Kim C, Fuke N, Martyn JA. Burn injury to rat increases nicotinic acetylcholine receptors in the diaphragm. *Anesthesiology* 1988; **68**: 401–6

10 Hinohara H, Morita T, Okano N, Kunimoto F, Goto F. Chronic intraperitoneal endotoxin treatment in rats induces resistance to d-tubocurarine, but does not produce up-regulation of acetylcholine receptors. *Acta Anaesthesiol Scand* 2003; **47**: 335–41

11 Fink H, Luppa P, Mayer B, *et al.* Systemic inflammation leads to resistance to atracurium without increasing membrane expression of acetylcholine receptors. *Anesthesiology* 2003; **98**: 82–8

12 Tsukagoshi H, Morita T, Takahashi K, Kunimoto F, Goto F. Cecal ligation and puncture peritonitis model shows decreased nicotinic acetylcholine receptor numbers in rat muscle: immunopathologic mechanisms? *Anesthesiology* 1999; **91**: 448–60

13 Witzemann V, Brenner HR, Sakmann B. Neural factors regulate AChR subunit mRNAs at rat neuromuscular synapses. *J Cell Biol* 1991; **114**: 125–41

14 Ibebunjo C, Martyn JAJ. Fiber atrophy, but not changes in acetylcholine receptor expression, contributes to the muscle dysfunction after immobilization. *Crit Care Med* 1999; **27**: 275–85

15 Fischer U, Reinhardt S, Albuquerque EX, Maelicke A. Expression of functional alpha7 nicotinic acetylcholine receptor during mammalian muscle development and denervation. *Eur J Neurosci* 1999; **11**: 2856–64

16 Osta WA, El-Osta MA, Pezhman EA, *et al.* Nicotinic acetylcholine receptor gene expression is altered in burn patients. *Anesth Analg* 2010; **110**: 1355–9

17 Fletcher GH, Steinbach JH. Ability of nondepolarizing neuromuscular blocking drugs to act as partial agonists at fetal and adult mouse muscle nicotinic receptors. *Mol Pharmacol* 1996; **49**: 938–47

18 Kopta C, Steinbach JH. Comparison of mammalian adult and fetal nicotinic acetylcholine receptors stably expressed in fibroblasts. *J Neurosci* 1994; **14**: 3922–33

19 Aosasa S, Ono S, Mochizuki H, *et al.* Mechanism of the inhibitory effect of protease inhibitor on tumor necrosis factor alpha production of monocytes. *Shock* 2001; **15**: 101–5

20 Nishiyama T, Hanaoka K. Do the effects of a protease inhibitor, ulinastatin, on elastase release by blood transfusion depend on interleukin 6? *Crit Care Med* 2001; **29**: 2106–10

21 Harvey A, Karlsson E. Protease inhibitor homologues from mamba venoms: facilitation of acetylcholine release and interactions with prejunctional blocking toxins. *Br J Pharmacol* 1982; **77**: 153–61

22 Rittirsch D, Huber-Lang MS, Flierl MA, Ward PA. Immunodesign of experimental sepsis by cecal ligation and puncture. *Nat Protoc* 2009; **4**: 31–6

23 Remick DG, Bolgos GR, Siddiqui J, Shin J, Nemzek JA. Six at six: interleukin-6 measured 6 h after the initiation of sepsis predicts mortality over 3 days. *Shock* 2002; **17**: 463–7

24 Osuchowski MF, Teener J, Remick D. Noninvasive model of sciatic nerve conduction in healthy and septic mice: reliability and normative data. *Muscle Nerve* 2009; **40**: 610–6

25 Van Den Bergh PYK, Piéret F. Electrodiagnostic criteria for acute and chronic inflammatory demyelinating polyradiculoneuropathy. *Muscle Nerve* 2004; **29**: 565–74

26 Cornblath DR, Mellits ED, Griffin JW, *et al.* Motor conduction studies in Guillain-Barre syndrome: description and prognostic value. *Ann Neurol* 1988; **23**: 354–9

27 Rannou F, Pennec JP, Rossignol B, *et al.* Effects of chronic sepsis on rat motor units: experimental study of critical illness polyneuromyopathy. *Exp Neurol* 2007; **204**: 741–7

28 Nayci A, Atis S, Comelekoglu U, *et al.* Sepsis induces early phrenic nerve neuropathy in rats. *Eur Respir J* 2005; **26**: 686–92

29 Wichterman KA, Baue AE, Chaudry IH. Sepsis and septic shock—a review of laboratory models and a proposal. *J Surg Res* 1980; **29**: 189–201

30 Hubbard WJ, Choudhry M, Schwacha MG, *et al.* Cecal ligation and puncture. *Shock* 2005; **24**(Suppl. 1): 52–7

31 Xiao H, Siddiqui J, Remick DG. Mechanisms of mortality in early and late sepsis. *Infect Immun* 2006; **74**: 5227–35

32 Narimatsu E, Nakayama Y, Sumita S, *et al.* Sepsis attenuates the intensity of the neuromuscular blocking effect of d-tubocurarine and the antagonistic actions of neostigmine and edrophonium accompanying depression of muscle contractility of the diaphragm. *Acta Anaesthesiol Scand* 1999; **43**: 196–201

33 Tomera JF, Martyn JA. Intraperitoneal endotoxin but not protein malnutrition shifts d-tubocurarine dose-response curves in mouse gastrocnemius muscle. *J Pharmacol Exp Ther* 1989; **250**: 216–20

34 Niiya T, Narimatsu E, Namiki A. Acute late sepsis attenuates effects of a nondepolarizing neuromuscular blocker, rocuronium, by facilitation of endplate potential and enhancement of membrane excitability in vitro. *Anesthesiology* 2006; **105**: 968–75

35 Lindstrom JM. Nicotinic acetylcholine receptors of muscles and nerves: comparison of their structures, functional roles, and vulnerability to pathology. *Ann N Y Acad Sci* 2003; **998**: 41–52

36 Kim CS, Arnold FJ, Itani MS, Martyn JA. Decreased sensitivity to metocurine during long-term phenytoin therapy may be attributable to protein binding and acetylcholine receptor changes. *Anesthesiology* 1992; **77**: 500–6

37 Han T, Kim H, Bae J, Kim K, Martyn JA. Neuromuscular pharmacodynamics of rocuronium in patients with major burns. *Anesth Analg* 2004; **99**: 386–92

38 Fambrough DM. Control of acetylcholine receptors in skeletal muscle. *Physiol Rev* 1979; **59**: 165–227

39 Wang H, Yang B, Han GW, Li ST. Potency of nondepolarizing muscle relaxants on muscle-type acetylcholine receptors in denervated mouse skeletal muscle. *Acta Pharmacol Sin* 2010; **31**: 1541–6

40 Chiodini F, Charpantier E, Muller D, *et al.* Blockade and activation of the human neuronal nicotinic acetylcholine receptors by atracurium and laudanosine. *Anesthesiology* 2001; **94**: 643–51

41 Placzek AN, Grassi F, Papke T, Meyer EM, Papke RL. A single point mutation confers properties of the muscle-type nicotinic acetylcholine receptor to homomeric alpha7 receptors. *Mol Pharmacol* 2004; **66**: 169–77

42 Rosenheimer JL. Factors affecting denervation-like changes at the neuromuscular junction during aging. *Int J Dev Neurosci* 1990; **8**: 643–54

43 Kim C, Martyn J, Fuke N. Burn injury to trunk of rat causes denervation-like responses in the gastrocnemius muscle. *J Appl Physiol* 1988; **65**: 1745–51

44 Winkelman C. Inactivity and inflammation: selected cytokines as biologic mediators in muscle dysfunction during critical illness. *AACN Clin Issues* 2004; **15**: 74–82

45 de Letter MA, Schmitz PI, Visser LH, *et al.* Risk factors for the development of polyneuropathy and myopathy in critically ill patients. *Crit Care Med* 2001; **29**: 2281–6

46 Eftimie R, Brenner HR, Buonanno A. Myogenin and MyoD join a family of skeletal muscle genes regulated by electrical activity. *Proc Natl Acad Sci USA* 1991; **88**: 1349–53

Handling editor: M. M. R. F. Struys